Catalysis Today 145 (2009) 236–242

Contents lists available at ScienceDirect

Catalysis Today

journal homepage: www.elsevier.com/locate/cattod

In situ structure–activity correlation experiments of the ruthenium catalyzed CO oxidation reaction

H. Over [a,*], O. Balmes [b], E. Lundgren [c]

[a] Physikalisch-Chemisches Institut, Justus Liebig University Giessen, Henrich Buff Ring 58, 35392 Giessen, Germany
[b] Beamline ID03, ESRF, Grenoble, France
[c] Department of Synchrotron Radiation Research, University of Lund, Sweden

ARTICLE INFO

Article history:
Available online 30 December 2008

Keywords:
Ru-oxide
CO oxidation
Kinetic data
Structure–activity correlation

ABSTRACT

The complex structure–activity correlation of the CO oxidation on ruthenium has been studied in a batch reactor by using in situ surface X-ray diffraction (SXRD) and on-line mass spectrometry. Two distinct active phases are identified at higher pressures in the mbar range depending on the reaction conditions: a non-oxidic phase and a RuO_2(1 1 0) layer of variable thickness ranging from 1.5 nm to 10 nm. For reaction temperatures lower than 520 K the experimental turnover frequency (TOF) numbers are shown to be almost identical for the two types of active phases. Above 520 K the RuO_2(1 1 0) layer turned out to be much more active than the non-oxidic phase. Kinetic reaction experiments on the RuO_2(1 1 0) phase reveal an activation energy of 78 ± 10 kJ/mol which is in perfect agreement with corresponding reactivity experiments on supported and powder RuO_2 catalyst. Under oxidizing reaction conditions and high concentration of CO_2 in the gas mixture, the RuO_2(1 1 0) model catalyst shows reversible product-poisoning.

1. Introduction

One of the major challenges met in (heterogeneous) catalysis research focuses on the identification of the active phase of the catalyst under practical reaction conditions. Frequently, the catalytically active phase is only stable under reaction conditions and may even change when the reactant mixture or the reaction temperature is varied. All these complications urgently call for in situ characterization of the catalytic system [1–11]. In order to have full access to the atomic scale structure of the catalyst one relies on the investigation of model catalysts with low structural complexity such as single crystalline films or single crystal surfaces.

The CO oxidation reaction is a prototype (model) reaction in surface chemistry. While the CO oxidation reaction itself is simple, the full system consisting of CO, O_2, and CO_2 in the gas phase together with the solid state catalyst may exhibit a quite complex reaction behavior. With in situ surface X-ray diffraction (SXRD) and on-line mass spectrometry, the complex structure–activity correlation in the CO oxidation on ruthenium has been elucidated. For the first time such experimental data are provided for the CO oxidation over the model catalyst RuO_2(1 1 0) and the non-oxidized Ru(0 0 0 1) surface for CO and O_2 pressures in mbar range. Quite surprisingly, the experimental turnover frequencies (TOFs) are practically identical for the non-oxidic Ru(0 0 0 1) phase and the RuO_2 phase when the temperature is below 520 K. Above 520 K the RuO_2(1 1 0) surface turned out to be much more active than the non-oxidic phase.

2. Experimental details

With the unique high-pressure chamber of ID03 at ESRF [12] we were able to follow simultaneously the surface structure of the Ru(0 0 0 1)-based model catalyst by surface X-ray diffraction (SXRD) and the reaction rate of the product formation (CO_2) via on-line mass spectrometry (MS) during the CO oxidation reaction over RuO_2(1 1 0) and non-oxidized Ru(0 0 0 1) under practical reaction conditions. The sample was mounted on a BN-encapsulated heater, the temperature was measured by a Re/W W5 thermocouple 2 mm away from the sample position on the heater plate. In the reaction experiments the high-pressure cell with a volume of about 0.8 dm^3 served as a batch reactor. Details about the design and properties of the batch reactor have been described in detail in the Ph.D. Thesis of Ackermann [13]. The chamber could be separated from the pumping system by a gate valve. By leaking the gas mixture from the batch reactor into the differentially pumped MS chamber, the gas composition was monitored on-line. The response of the mass spectrometer to a change of the gas composition in the reaction cell is <5 s. For SXRD, a photon energy of 17 keV was selected with a Si(1 1 1) monolithic channel cut monochromator corresponding to a wave length of 0.73 Å.

* Corresponding author. Tel.: +49 641 9934550; fax: +49 641 9934559.
E-mail address: Herbert.Over@phys.chemie.uni-giessen.de (H. Over).
URL: http://www.uni-giessen.de/cms/fbz/fb08/chemie/physchem/ag-prof-dr-herbert-over

0920-5861/$ – see front matter © 2008 Elsevier B.V. All rights reserved.
doi:10.1016/j.cattod.2008.10.048

In reciprocal space, **H** and **K** are the in-plane lattice vectors corresponding to the in plane lattice vectors $\mathbf{A_1}$ and $\mathbf{A_2}$ of the Ru(0 0 0 1) surface (with a length of 2.71 Å), and **L** is the reciprocal out-of-plane vector corresponding to $\mathbf{A_3}$ (with a length of 4.28 Å). The reciprocal lattice vectors of the tetragonal RuO_2(1 1 0) on Ru(0 0 0 1) are given in fractions of **H**, **K** and **L**, and are referred to as **h**, **k**, and **l**, where **h** is parallel to **H** and **k** is equivalent to the **H** + **K** (by mirror plane symmetry) direction (cf. Fig. 1a) while **l** is aligned along the **L** direction. For more details the reader is referred to Ref. [14]. A typical **h**-scan of the non-oxidic and the oxide phase are shown in Fig. 1b. The RuO_2(1 1 0) oxide reveals a diffraction peak at **h** = 0.73, while the peak at **h** = 1.0 is related to diffraction from the Ru(0 0 0 1) substrate.

The Ru(0 0 0 1) sample was prepared by Ar-ion etching (U = 2 kV, I = 15 mA, p(Ar) = 10^{-5} mbar, for 20 min at 760 K) and oxygen treatment cycles at elevated temperatures. The structure–activity experiments were performed by exposing the sample to various O_2 and CO gas mixtures with partial pressures ranging from some 100 Pa to 3×10^4 Pa and varying CO/O_2 concentration ratios at sample temperature ranging from 400 K to 800 K. In a typical experiment a mixture of CO and O_2 was admitted into the batch reactor and then the sample was brought to its actual reaction temperature. At the beginning of an experiment, the sample could be prepared in the non-oxidic state or could be covered with a layer of oxide of varying thickness. When the reaction experiment was terminated, the residual gas mixture in the chamber was pumped out, and the sample re-prepared.

3. Results and discussion

3.1. General remark to the analysis of the kinetic reaction data

The quadrupole mass spectrometer (QMS) signals for O_2, CO and CO_2 are translated to corresponding partial pressures in the batch reactor. The CO and O_2 partial pressures are calibrated by the pressure gauge reading, when filling the batch reactor with CO and O_2. Accounting for the slightly different ionization probabilities of CO and CO_2, we can determine the CO_2 partial pressure from the measured OMS signals.

The evolution of the partial pressures of CO and O_2 with reaction time is determined by the chemical equation, i.e. $CO + (1/2)O_2 \rightarrow CO_2$. This means that the partial pressure of CO decreases twice as fast as that of O_2 in the course of the reaction. Only for an ideal stoichiometric O_2/CO mixture of 1:2, the reactant ratio in the batch reactor is constant during the reaction. As soon as the gas mixture is $P(O_2):P(CO) > 1/2$ the ratio will increase with reaction time until all CO is consumed. For a starting condition with a reactant ratio $P(O_2):P(CO) < 1/2$ the ratio decreases further during the reaction until all O_2 is consumed.

From the CO_2 partial pressure we can derive the turnover frequency (TOF), which is defined as the number of produced CO_2 molecules per active site and second. The TOF is calculated from the following formula:

$$\mathrm{TOF} = \frac{VL}{RT}\frac{1}{\#\,\mathrm{Cat}}\frac{dP(\mathrm{CO_2})}{dt} \quad (1)$$

with V = volume of the batch reactor (0.8 dm^3), L = Avogadro's number = 6.022×10^{23} 1/mol, R = general gas constant = 8.4135 J/(k mol), T = gas temperature = 300 K, #Cat = number of active catalyst sites = 10^{15} (the sample area is 1 cm^2).

Since in a batch reactor both partial pressure of CO and O_2 decline with the reaction time and the TOF is given for particular partial pressures of the reaction mixture, it is useful to define a normalized $(TOF)_{norm}$:

$$(\mathrm{TOF})_{\mathrm{norm}} = \frac{\mathrm{TOF}}{P(\mathrm{CO})\sqrt{P(\mathrm{O_2})}} \quad (2)$$

which compensates for the nominal pressure dependence of TOF when the reaction order is assumed to be 1 and 1/2 in CO and O_2, respectively.

Some critical comments on the use of the present batch reactor for determining TOF values are in place. The batch reactor is not running under isothermal conditions, i.e. the gas and model catalyst surface temperatures are different. Most of the gas molecules are close to room temperature (temperature of the chamber walls), while the sample can be heated deliberately to the desired temperature. This results in an uncertainty in the actual gas temperature T entering Eq. (1). In the calculation of the TOF values mass transfer limitations are also not accounted for. Both shortcomings will affect the derived TOF values irrespective of the catalytically active phase under consideration. Therefore a direct comparison of the activity of the oxidic phase with that of the non-oxidic phase on Ru(0 0 0 1) under identical reaction conditions will provide firm conclusions about which of the phases is the more active one.

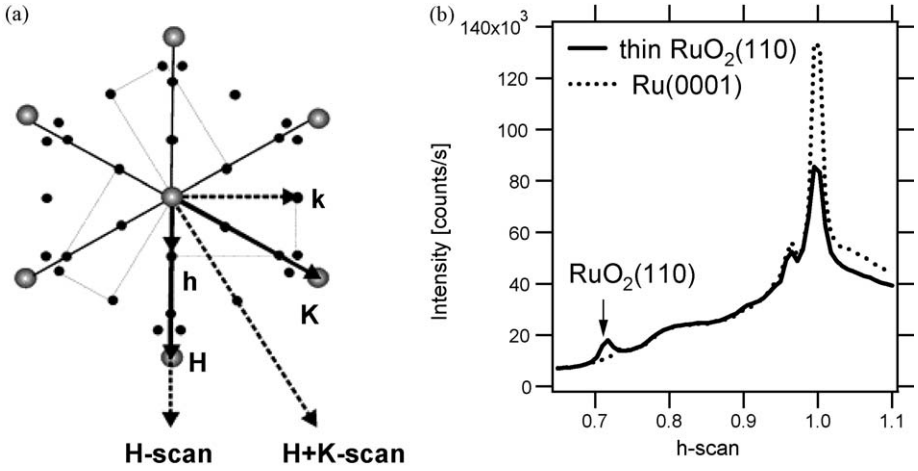

Fig. 1. (a) Schematic LEED pattern of Ru(0 0 0 1) (open discs) and RuO_2(1 1 0) (small solid discs). In reciprocal space the in-plane high-symmetry direction is denoted by **H**, **H** + **K** for Ru(0 0 0 1) and **h**, **k** for RuO_2(1 1 0) and (b) **h**-scans at **l** = 0.3 of clean Ru(0 0 0 1) in comparison to a RuO_2(1 1 0) coated Ru(0 0 0 1) surface.

3.2. Example for a complex structure–reactivity correlation in the CO oxidation on ruthenium

In this section we present a specific set of experiments illustrating the complex structure–activity correlation for the CO oxidation over the RuO_2(1 1 0)/Ru(0 0 0 1) model catalyst [15]. A 1.6 nm thick RuO_2(1 1 0) film on Ru(0 0 0 1) was prepared prior to the actual reaction experiments by exposing the Ru(0 0 0 1) surface to 1000 Pa of O_2 at 640 K. The sample was then cooled to 350 K and additional 1800 Pa of CO was admitted to the (batch) reaction cell. Subsequently the reaction temperature was raised stepwise up to 720 K over a time period of 2800 s (cf. Fig. 2a). At temperatures up to 500 K (regions A–C in Fig. 2a), the structure of the oxide film does not change as indicated by the repetitive **h**-scans in Fig. 2a; the peak intensity at **h** = 0.73 is uniquely related to the RuO_2(1 1 0) oxide surface [14].

For T = 350 K, almost no CO_2 is formed (cf. Fig. 2b). Above 400 K the CO_2 production is accelerated, revealing a constant TOF of 95 l/s (at 400 K) which increases to 190 l/s on raising the temperature to 450 K. Both CO and O_2 are continuously consumed during the CO oxidation, but the stoichiometry of the reaction feed is nearly preserved during the first 2200 s as indicated in Fig. 2c. In region C (1000s–1600s), the CO_2 production stops, although the temperature is increased to 500 K and no apparent modification in the structure of the active state occurs. Presumably the catalyst deactivates whose origin is not well understood.

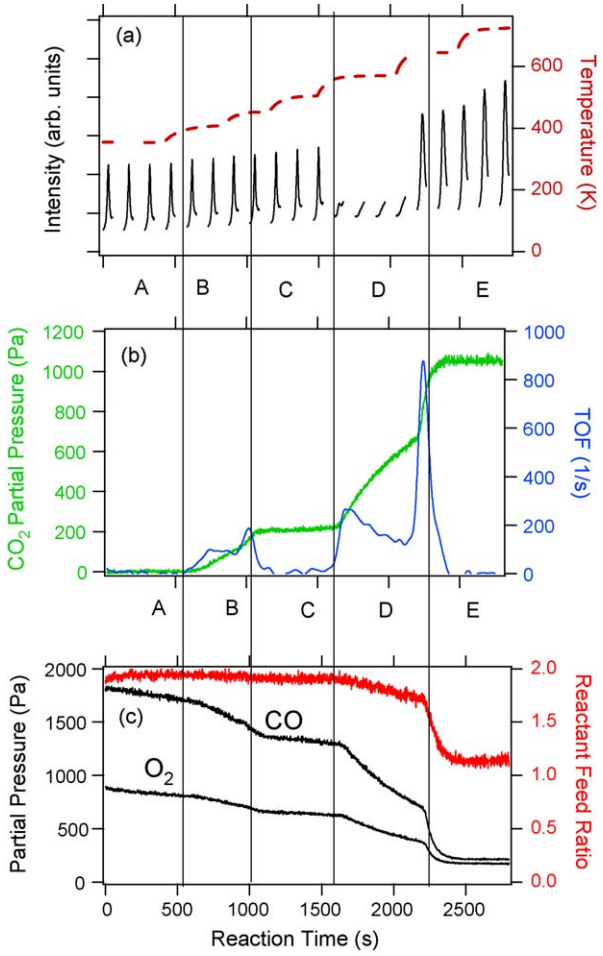

Fig. 2. The reaction cell is run as a batch reactor and both structural and reactive properties are monitored in situ by SXRD and on-line mass spectrometry, respectively, during the CO oxidation reaction over RuO_2(1 1 0)/Ru(0 0 0 1). (a) Temperature protocol (brown) as a function of the reaction time. Repetitive **h**-scans at **l** = 0.3 around a RuO_2(1 1 0) related reflection (**h** = 0.73), monitoring the oxide structure during the CO oxidation reaction. (b) Quantification of the CO_2 production using mass spectrometry translated into CO_2 partial pressure in the gas mixture. From the CO_2 partial pressure the turnover frequency (TOF) is derived. (c) Partial pressures of O_2 and CO during the CO oxidation reaction over RuO_2(1 1 0)/Ru(0 0 0 1). The red trace shows the O_2/CO ratio of the reaction mixture. (For interpretation of the references to color in this figure legend, the reader is referred to the web version of the article.)

At the end of region C (reaction time about 1600 s), the oxide film disappeared. Increasing the temperature to 570 K, the RuO_2(1 1 0) surface is completely reduced, followed by a substantial increase of the activity: TOF = 260 l/s. The CO and O_2 partial pressures decrease rapidly, increasing the reactant ratio $P(O_2)/P(CO)$ significantly above 0.5. When the temperature was further increased to 640 K, the oxide state reappeared (with significantly higher diffraction intensity at **h** = 0.73). Obviously the remaining reactant mixture in the batch reactor is now net oxidizing. From corresponding **l**-scans at h = 0.73 we derive a thickness of the RuO_2(1 1 0) film of 2.3 nm. The oxidation process of Ru(0 0 0 1) is accompanied by a sudden rise of the TOF value to 850 l/s. With this increase of TOF the O_2/CO stoichiometry of the reactant feed increases significantly from 0.6 to 0.87, i.e. the reaction mixture is now much more oxidizing than during the first 2000 s (cf. Fig. 2c, red trace). Beyond the maximum the TOF declines rapidly. Practically the CO oxidation reaction stops, although both CO (210 Pa) and O_2 (170 Pa) are still present in the gas mixture. A further increase of the temperature to 720 K is not able to restore the activity of the RuO_2(1 1 0) catalyst.

Already this particular experiment may illustrate the complex structure–activity relationship in the seemingly simple CO oxidation over RuO_2(1 1 0)/Ru(0 0 0 1). The activity of the catalyst increases substantially whenever the catalyst undergoes structural changes either by reducing RuO_2(1 1 0) or by forming RuO_2(1 1 0). At a temperature of 400 K, the (metastable) oxide catalyst works stably with a medium high activity. Deactivation of the catalyst appears in the temperature region of 450–500 K. Chemical reduction of the oxide recovers the catalytic activity. When the Ru(0 0 0 1) surface re-oxidized the activity increased steeply. Complete deactivation is observed above 650 K and under strongly oxidizing reaction conditions ($P(O_2)/P(CO)$ = 0.87) and a high partial pressure of CO_2. In the following we present detailed in situ experiments to elucidate this complex structure/reactivity behavior.

3.3. Kinetics of the CO oxidation reaction on various active states of ruthenium

In this section we deal with the reaction kinetics of the CO oxidation. In all experiments the gas mixture was admitted to the reaction chamber (batch reactor) first and then the sample temperature was raised to the desired temperature. In Fig. 3 we present representative examples of reactivity data at about T = 530 K for the two distinct states, namely the non-oxidic phase and the RuO_2(1 1 0) layer. Kinetic data for other temperatures are summarized in Fig. 4 in the form of an Arrhenius plot. The temperature ramp from room temperature to 530 K is reflected by the steep rise of the TOF during the first 200 s. During the reactivity experiments the surface structure was continuously monitored.

For the particular reaction temperature of 525 K respectively 540 K, the **h**- and **l**-scans of the respective surface structures are shown in Fig. 3. For both active surface terminations (non-oxidic and oxidic phase) the **h**- and **l**-scans did not vary with the reaction temperature.

After 200 s the CO and O_2 partial pressures decrease with reaction time, while the CO_2 partial pressure increases. As seen in Fig. 3a the time variation of TOF for the non-oxidic phase follows closely that of the CO partial pressure with reaction time,

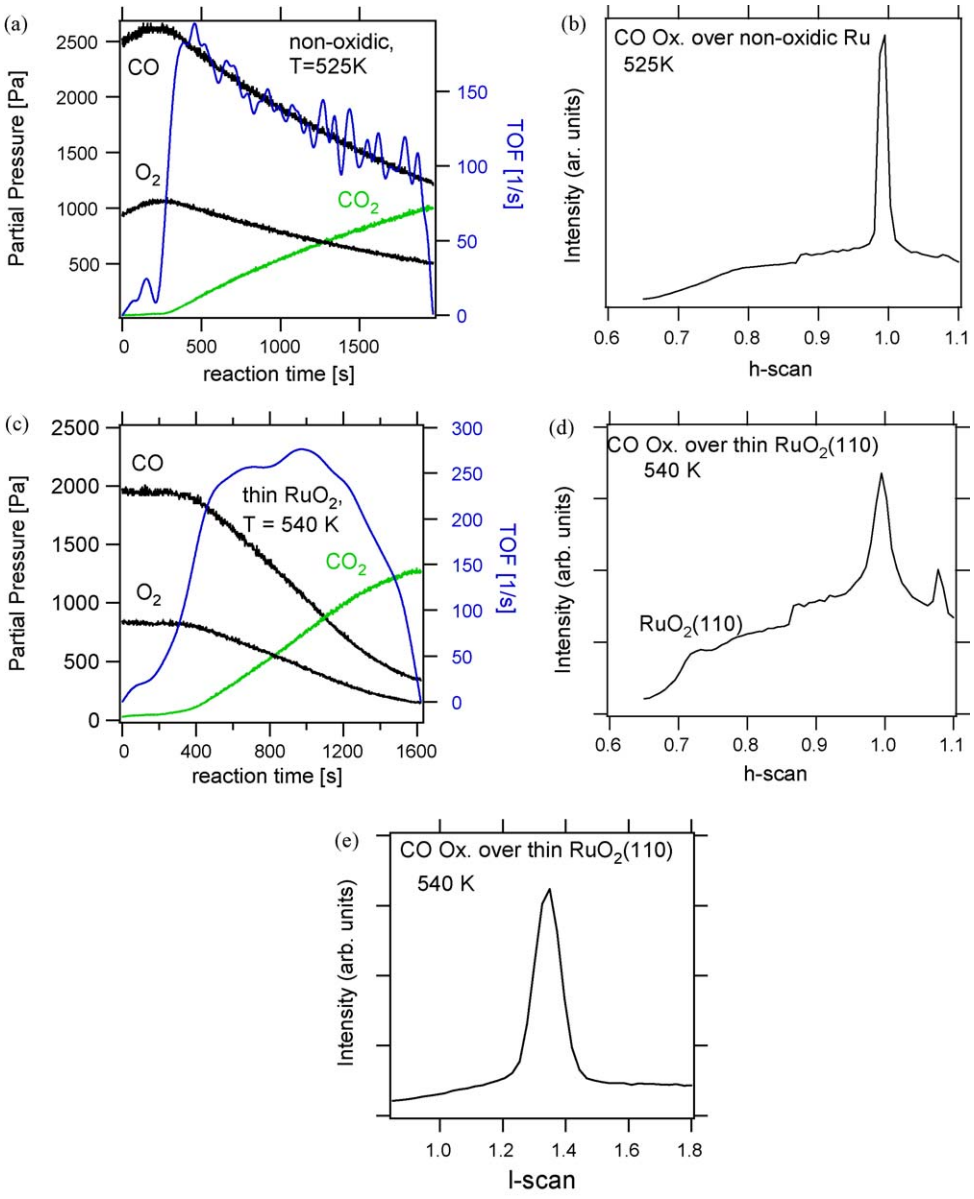

Fig. 3. Reactivity data for the CO oxidation: $P(CO)$, $P(O_2)$, $P(CO_2)$ and TOF as a function of the reaction time. At $t = 0$ s the heating ramp started, increasing the sample temperature to final temperature T_{final} within 200 s. (a) Non-oxidic state: $T_{final} = 525$ K, at the beginning: $P(CO) = 2500$ Pa, $P(O_2) = 1000$ Pa. (c) Thin $RuO_2(1\,1\,0)$ oxide: $T_{final} = 540$ K, at the beginning: $P(CO) = 2000$ Pa, $P(O_2) = 800$ Pa. The surface structure was monitored in situ by SXRD: (b) **h**-scan of the non-oxidic phase; (d) and (e) **h**-scan (at **l** = 0.3) and **l**-scan (at **h** = 0.73) of the oxidic phase.

suggesting a first order reaction in CO and zero order in O_2. This behavior has also been observed by Peden and Goodman [16] for the "(1×1)O" phase. We presume therefore that the active phase of Peden and Goodman and the non-oxidic phase studied here are identical. The highest TOF reached at 525 K is 170 l/s just at the beginning of the reaction. The corresponding **h**-scan in Fig. 3b indicates high diffraction intensity at the **h** = 1 position, but no intensity at **h** = 0.73 as expected for the non-oxide phase. Very similar **h**-scans were measured (but not shown) for other reaction temperatures up to 670 K.

Specific reactivity data of $RuO_2(1\,1\,0)$ for a reaction temperature of 540 K are shown in Fig. 3c. The maximum TOF is 250 l/s and this TOF does not vary with the partial pressures of both CO and O_2 over a wide pressure range. This indicates zero reaction order in CO and O_2. The corresponding **h**-scan in Fig. 3d indicates $(1\,1\,0)$-oriented RuO_2 as indicated by diffraction maxima at **h** = 0.73 and 1.08 is observed. From the **l**-scan at **h** = 0.73 (cf. Fig. 3e) the thickness of the oxide is determined to be 5 nm. Very similar **h**- and **l**-scans were measured for other reaction temperatures up to 670 K, indicating that the oxide phase is stable under these reaction conditions with a constant oxide thickness of 5 nm. We should mention that the first reaction experiment with $RuO_2(1\,1\,0)$ was performed at 670 K, all subsequent experiments were performed at lower temperatures down to 470 K.

The reaction orders of RuO_2 and the non-oxidic phase differ substantially. Below 530 K, the reaction on RuO_2 proceeds with zero order in CO and O_2, while above 560 K the reaction order in CO is one and in O_2 one half. The zero reaction order for RuO_2 was also observed for powder RuO_2 at reaction temperatures in the range from 393 K to 453 K [17]. For the non-oxidic phase the CO oxidation reaction proceeds for the temperature range 500–640 K with first order in CO and zero order in O_2. We should note that the reaction order was not determined in the standard way, where both O_2 and CO partial pressures are varied independently, but rather both partial pressures are varied in a coupled way by the ongoing reaction.

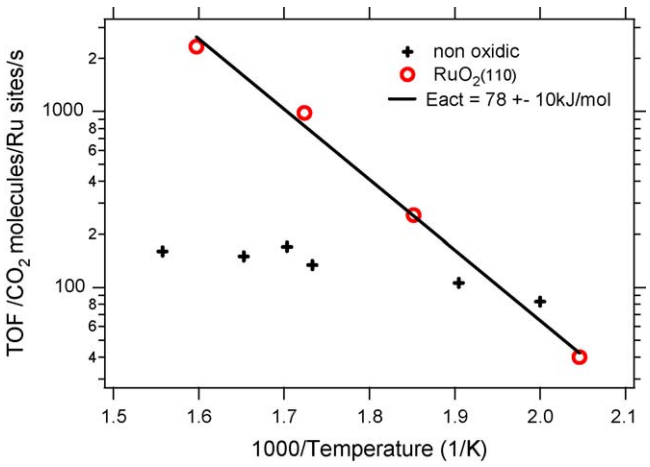

Fig. 4. TOF data for varying sample temperatures represented in an Arrhenius plot. The reaction data were selected so that in all measurements the $P(CO)$ partial pressure was 1400 Pa and the partial pressure of O_2 was 550 Pa. For the case of $RuO_2(1\,1\,0)$ the activation barrier was determined to be 78 ± 10 kJ/mol.

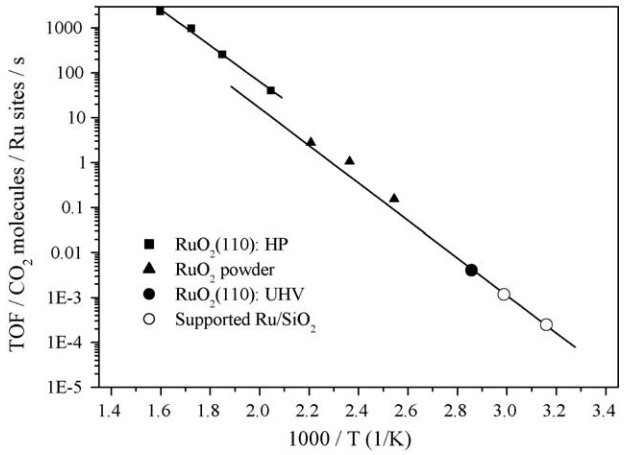

Fig. 5. Arrhenius plot of turnover frequencies TOF (CO_2 molecules formed per Ru site and second) measured for the oxidation of CO over RuO_2 powder [17] (filled triangle), supported RuO_2 on SiO_2 [19] (open circles), UHV experiment on $RuO_2(1\,1\,0)$/Ru(0 0 0 1) [18] (filled circle). For these systems the determined activation energy was 82 kJ/mol [17]. These TOF data from the literature are compared to those for $RuO_2(1\,1\,0)$ in the 1000 Pa pressure range (HP: filled squares) which yield an activation energy of 78 ± 10 kJ/mol.

With similar reactivity data as shown in Fig. 3 for various other temperatures ranging from 470 K to 670 K, we determined the TOF values for a specific set of partial pressures, namely $P(CO)$ = 1400 Pa and $P(O_2)$ = 550 Pa. Identical reaction conditions allow for a direct comparison of the TOF data in Fig. 4 for the two catalytically active states considered without facing the problem of differing reaction order and the shortcomings of the used batch reactor (cf. discussion in Section 3.1). Surprisingly in the low temperature region below 550 K the TOF values are practically identical for the two active states of the model catalyst. This finding is consistent with a previous compilation of TOF values for model and supported Ru catalyst [17]. Above a reaction temperature of 550 K the non-oxidic state is much less active than the oxidic phase (cf. Fig. 4).

For the non-oxidic phase the TOF saturates and decreases for temperatures above 550 K similar to Peden and Goodman's [16] experiments. Above 550 K $RuO_2(1\,1\,0)$ is much more active than the non-oxidic phase. The $RuO_2(1\,1\,0)$ layer achieves a TOF value of 2330 l/s at 630 K, while the maximum TOF for the non-oxidic phase is only 160 l/s accomplished at 570 K.

From the temperature-dependent TOF data of the $RuO_2(1\,1\,0)$ surface an activation barrier for CO oxidation is determined to be 78 ± 10 kJ/mol. The large uncertainty of ±10 kJ/mol is due essentially to the temperature uncertainty of ±10 K. The activation energy of 78 ± 10 kJ/mol is in perfect agreement with activation energies found on supported and powder Ru-based catalysts [17], however, deviating substantially from an activation energy determined on the basis of previous temperature-dependent UHV experiments in a very limited temperature interval [18].

In Fig. 5 the TOF values of $RuO_2(1\,1\,0)$ are directly compared to values published in the literature, namely with TOF values for supported RuO_2 [19] and powder RuO_2 [17], as well as with a previous UHV experiment on $RuO_2(1\,1\,0)$ [18]. It is quite surprising that all these values fit remarkably well a single Arrhenius curve with an activation energy of about 80 kJ/mol. There is only a small rigid shift of the high-pressure data on $RuO_2(1\,1\,0)$ to higher TOF values which may be related to the non-isothermal conditions in the used batch reactor (cf. Section 3.1). The impressive overall agreement among the various catalytic systems in Fig. 5 indicates that the material's gap has successfully been bridged for the CO oxidation reaction on RuO_2. For all three kinds of RuO_2-based catalyst in a similar pressure range of 1000 Pa, the temperature-dependent TOF values yield a unique activation energy. From the kinetic data in Fig. 5 one may even speculate that the pressure gap is bridged for $RuO_2(1\,1\,0)$ from UHV to 1000 Pa. However, this conclusion is only based on a single UHV experiment.

3.4. Deactivation of $RuO_2(1\,1\,0)$ catalyst

Deactivation of the model catalyst in the CO oxidation reaction has not been observed for the non-oxidic phase. However, RuO_2 reveals deactivation in the CO oxidation reaction under specific reaction conditions, namely under net oxidizing reaction conditions and with substantial concentration of CO_2 present in the reaction mixture.

A particular reaction experiment is compiled in Fig. 6, where the sample temperature was increased from room temperature to 673 K in a gas mixture consisting of $P(CO)$ = 1600 Pa and $P(O_2)$ = 700 Pa. With SXRD it is shown that the structure of the oxide surface does not change appreciably. Only the thickness of the oxide increased somewhat. The TOF increases steeply with reaction time due to the rise in reaction temperature. The maximum TOF is reached with 2200 l/s at t = 400 s. Subsequently the TOF decreases steeply, much faster than the CO and O_2 partial pressure drop.

In Fig. 6, we show the normalized TOF, i.e. the TOF is normalized to the formal reaction order $P(CO)\sqrt{P(O_2)}$. During the decline of TOF within the first 100 s the normalized TOF is practically constant, i.e. the TOF decline within this time period is solely determined by the decrease in the partial pressure of the reactants CO and O_2 in the course of the reaction. However, beyond a reaction time of 600 s, even the normalized TOF drops to zero, indicating that besides a diminishing of the reactant partial pressures a second process is operative to reduce the TOF. At t = 700 s, the TOF is practically zero, although the partial pressures of CO and O_2 are still appreciable ($P(CO)$ = 150 Pa and $P(O_2)$ = 100 Pa). Obviously the catalyst is facing poisoning.

The deactivation of $RuO_2(1\,1\,0)$ is reversible as shown by the following experiment. We ran the first reaction experiment with $P(CO)$ = 2000 Pa and $P(O_2)$ = 850 Pa. After increasing the temperature to 626 K, the TOF went up to a maximum of 2400 l/s and subsequently declined until it reaches zero at t = 700 s (cf. Fig. 7, left). Since the partial pressures $P(CO)$ and $P(O_2)$ are still quite high a vanishing TOF indicates deactivation of the catalyst. Subsequently we reduced the temperature to room temperature, evacuated the reaction cell and admitted again a fresh CO + O_2

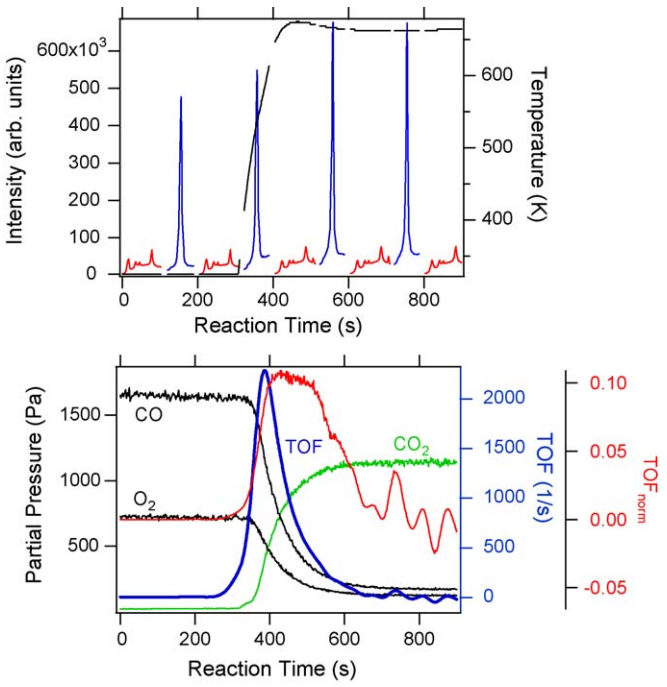

Fig. 6. Structure/activity experiments for the CO oxidation over RuO_2(1 1 0). The reaction mixture consists of $P(CO) = 1700$ Pa and $P(O_2) = 750$ Pa. The sample temperature is then increased from room temperature to 673 K. Repetitive **h**-scans (**l** = 0.3) and **l**-scans (**h** = 0.73) are shown in the top panel. The reactivity measurements are summarized in the bottom panel. The partial pressure of CO, O_2 and CO_2 are shown as a function of reaction time. When the temperature reaches 673 K, the maximum TOF is accomplished. The normalized TOF indicates that deactivation of the RuO_2 catalyst sets in after 500 s.

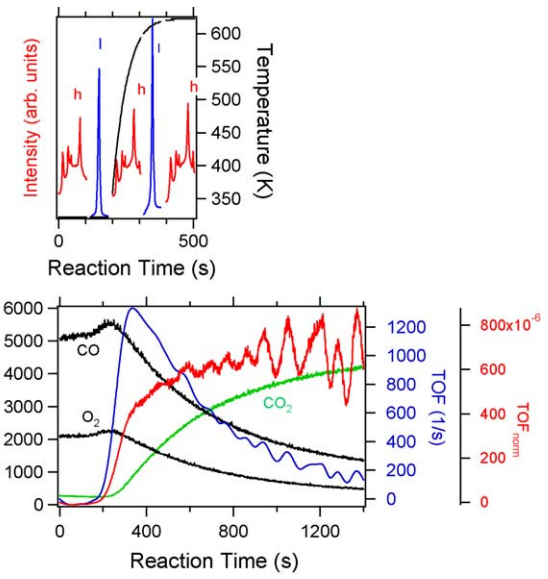

Fig. 8. Structure/activity experiments for the CO oxidation over RuO_2(1 1 0). The reaction mixture consists of $P(CO) = 5000$ Pa and $P(O_2) = 2000$ Pa. The sample temperature is then increased from room temperature to 620 K. Repetitive **h**- and **l**-scans are shown in the top panel. The partial pressures of CO, O_2 and CO_2 are shown in the bottom panel as a function of reaction time. When the temperature reaches 600 K, the maximum TOF is accomplished. The normalized TOF indicates no deactivation of the RuO_2 catalyst.

mixture with practically identical partial pressures as for the first reaction experiment. As seen in Fig. 7 (right) the activity of the catalyst is restored and subsequently a similar as in Fig. 7 (left) deactivation process occurs with the RuO_2(1 1 0) catalyst. From these experiments we conclude that the deactivation process is reversible.

This deactivation process is only observed if the reaction mixture is net oxidizing and the CO_2 partial pressure in the batch reactor is sufficiently high. We presume that the product CO_2 is forming a carbonate species on the oxygen-covered RuO_2(1 1 0) surface, which in turn causes a reversible deactivation. When the reactor is evacuated and annealed to 673 K in a pure $CO + O_2$ reaction mixture, the carbonate species decompose, restoring the original activity of RuO_2(1 1 0). Recently Rössler et al. [20] have proposed that such a carbonate species is stable up to 600 K. In these experiments the oxide surface was exposed to pure O_2 of 1×10^4 Pa. With STM the formation of a $c(2 \times 2)$ surface was observed which passivates the surface, leading to a complete catalytic deactivation at 300 K. From TDS and XPS Rössler et al. concluded that a carbon containing species causes this passivation, presumably a strongly bound carbonate species.

In Fig. 8, we present similar reaction experiments as in Fig. 7 with a net reducing reaction mixture. SXRD indicates again that the active state of the catalyst is RuO_2(1 1 0) and only slight changes in the thickness of the oxide occur during the reaction. The sample temperature is raised from room temperature to 620 K in a reaction mixture consisting of $P(CO) = 5000$ Pa and $P(O_2) = 2000$ Pa. The TOF increases initially due to the temperature raise, reaching a maximum of 1200 l/s after $t = 380$ s. The subsequent decline of TOF is solely due to the diminishing CO and O_2 partial pressures, as indicated by a constant value of the

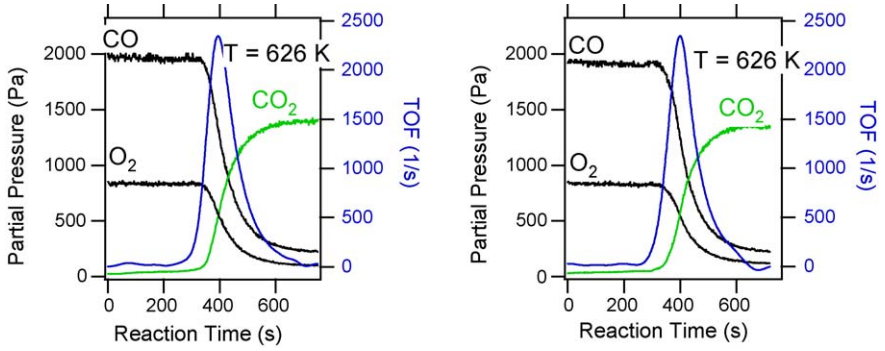

Fig. 7. Reversibility of deactivation of RuO_2(1 1 0) during CO oxidation under oxidizing reaction conditions. Both experiments used a reaction mixture consisting of $P(CO) = 2000$ Pa and $P(O_2) = 850$ Pa (left). In the first reaction experiment, the sample temperature was increased from room temperature to 626 K. The partial pressures of CO, O_2 and CO_2 are shown as a function of reaction time. When the temperature reaches 626 K, the maximum TOF is accomplished followed by a steep decline. After $t = 650$ s the TOF is practically zero, indicating deactivation of the catalyst (right). After the first reaction experiment was completed, the sample was cooled to room temperature, the gas mixture was pumped out and the chamber was again filled with the same $CO + O_2$ mixture as before. Subsequently, the sample temperature was increased from room temperature to 626 K to start the second reaction experiments.

normalized TOF. Obviously, no significant deactivation takes place under reducing reaction conditions. We may note that product-poisoning might not occur under more realistic conditions where a flow reactor is deployed.

4. Concluding remarks

The complex structure–activity correlation in the CO oxidation on ruthenium has been studied in a batch reactor applying the technique of in situ surface X-ray diffraction (SXRD) and on-line mass spectrometry. The catalytic system, consisting of CO, O_2 and CO_2 in the gas phase and the Ru(0 0 0 1) single crystalline model catalyst, reveals two distinct active phases at higher pressure in 1000 Pa range depending on the specific reaction conditions: a non-oxidized phase and RuO_2(1 1 0). Both active states are stable over a wide pressure and temperature range. For both phases we have performed reactivity experiments while in situ monitoring structure of the catalytic state. Surprisingly, below a reaction temperature of 520 K the experimental TOF numbers are almost identical for the two types of active phases. Above 520 K RuO_2(1 1 0) turned out to be much more active than the non-oxide phase. The pressure dependence of the two catalytic phases reveals distinct differences as well. The CO oxidation over the non-oxidic phase proceeds first order in CO and zero order in O_2. The CO oxidation over RuO_2 shows at higher temperature first and half order kinetics in CO and O_2, respectively and zero order at temperatures below 540 K. Under strongly oxidizing conditions and high concentration of CO_2, the RuO_2(1 1 0) state discloses product-poisoning, i.e. reversible deactivation of the catalyst probably by carbonate formation. This product-poisoning does not occur under reducing reaction conditions.

Acknowledgements

HO thanks for the financial support from the German Science foundation and EL financial support from the Swedish Research Council. Support by the ESRF staff is gratefully acknowledged.

References

[1] A. Stierle, A. Moelenbrok, MRS Bull. 32 (2007) 1000.
[2] E. Lundgren, H. Over, J. Phys. Condens. Matter 20 (2008) 180302.
[3] S. Ferrer, M.D. Ackermann, E. Lundgren, MRS Bull. 32 (2007) 1010.
[4] M.D. Ackermann, T.M. Pedersen, B.L.M. Hendriksen, O. Robach, S.C. Bobaru, I. Popa, C. Quiros, H. Kim, B. Hammer, S. Ferrer, J.W.M. Frenken, Phys. Rev. Lett. 95 (2005) 255505.
[5] R. Westerström, J.G. Wang, M. Ackermann, J. Gustafson, A. Resta, A. Mikkelsen, J.N. Andersen, E. Lundgren, O. Balmes, X. Torrelles, J.W.M. Frenken, B. Hammer, J. Phys. Condens. Matter 20 (2008) 184018.
[6] P.L. Hansen, S. Helveg, J.R. Rostrup-Nielsen, B.S. Clausen, H. Topsøe, Science 295 (2002) 2053.
[7] R. Blume, M. Hävecker, S. Zafeiratos, D. Teschner, E. Kleimenov, A. Knop-Gericke, R. Schlögl, A. Barinov, P. Dudin, M. Kiskinova, J. Catal. 239 (2006) 345.
[8] B.L.M. Hendriksen, S.C. Bobrau, J.W.M. Frenken, Surf. Sci. 552 (2004) 229.
[9] C.R. Henry, Surf. Sci. Rep. 31 (1998) 231.
[10] M.A. Newton, A.J. Dent, S.G. Fiddy, B. Jyoti, J. Evans, Catal. Today 126 (2007) 64.
[11] G. Rupprechter, Catal. Today 126 (2007) 3.
[12] P. Bernhard, K. Peters, J. Alvarez, S. Ferrer, Rev. Sci. Instrum. 70 (1999) 1478.
[13] M.D. Ackermann, Ph.D. Thesis, Kamerlingh Onnes Laboratory, Leiden University, Leiden, The Netherlands, 2007.
[14] Y.B. He, M. Knapp, E. Lundgren, H. Over, J. Phys. Chem. B 109 (2005) 21825.
[15] H. Over, Y.D. Kim, A.P. Seitsonen, S. Wendt, E. Lundgren, M. Schmid, P. Varga, A. Morgante, G. Ertl, Science 287 (2000) 1474–1476.
[16] C.H.F. Peden, D.W. Goodman, J. Phys. Chem. 90 (1986) 1360.
[17] J. Assmann, V. Narkhede, N.A. Breuer, M. Muhler, A.P. Seitsonen, M. Knapp, D. Crihan, A. Farkas, G. Mellau, H. Over, J. Phys. Condens. Matter 20 (2008) 184017.
[18] J. Wang, C.Y. Fan, K. Jacobi, G. Ertl, J. Phys. Chem. B 106 (2002) 3422–3427.
[19] J. Assmann, E. Löffler, A. Birkner, M. Muhler, Catal. Today 85 (2003) 235.
[20] M. Rössler, S. Günther, J. Wintterlin, J. Phys. Chem. C 111 (2007) 2242.